Short communication

Modeling of kinetic behavior of the lead dioxide electrode in a lead–acid battery by means of electrochemical impedance spectroscopy

M. Hejabi [a,*], A. Oweisi [a], N. Gharib [b]

[a] *Research and Development Center, Niru Battery Manufacturing Company, Tehran, Iran*
[b] *Vehicle, Fuel and Environment Research Institute, University of Tehran, Tehran, Iran*

Abstract

In this paper a mathematical model for the electrochemical impedance of a positive electrode in the lead–acid battery was developed. The mechanisms of the electrode processes involved in the batteries were obtained from the literature. Having selected the rate-controlling step as well as the fast reversible (equilibrated) and irreversible steps, we embarked on the formulation of *I*–*V* behavior using Butler–Volmer and Fick's law for charge and mass transfer process, respectively. The equivalent circuit consists of resistors, capacitors and mass transfer elements. Each electrical element expresses physico-chemical parameters such as diffusion coefficient, concentration, rate constant, etc. So, impedance plots can be used to determine the effects of each parameter on the performance of the cells. The simulation model also shows that the state-of-charge (SOC) plays an important role in the Nyquist plot of the positive electrode. Model results are compared with experimental results for cell potential and different SOC.
© 2005 Elsevier B.V. All rights reserved.

Keywords: Lead–acid battery; Positive plate; Modeling; Impedance spectroscopy; Nyquist plot

1. Introduction

The lead–acid battery has been used widely as a secondary battery for almost 150 years, since its invention by Planté in 1859 [1,2]. The advantages of the lead–acid system are its excellent high-rate discharge capability, good specific energy, high reliability robustness, low cost in both manufacturing and recycling, as they are manufactured mainly from a single low-cost raw material [3,4].

Impedance measurements are widely used to analyze the interfacial process, the variation in the internal resistance, the state-of-charge and the residual capacity of lead–acid batteries. This method is accurate, fast and non-destructive in nature [5–7].

The impedance study of lead–acid batteries is beset by difficulties that are caused by the complex nature of the process involved. From the system point of view, the batteries are non-linear, multi-parameters, quasi-irreversible, large statistical systems with distributed parameters on both the macro- and

micro-scale. Processes of energy and mass transport take place in the batteries that cause significant changes in the internal microstructure and operational behavior [8,9].

The model development history of lead–acid battery starts from late 1950s [10,11]. Nguyen et al. proposed a model for discharge, rest and charge to lead–acid battery and they introduced SOC as a dynamic parameter in the model [13]. Tenno proposed a model for overcharging of a battery. The model covers the full discharge–recharge cycle including deep discharge and overcharge. His modified model contains new formula for electrode morphology, applying charging factor to SOC, electrode porosity and acid concentration [10]. Mauracher and karden develop a battery model that gives the terminal voltage as a function of current and time. Their model structure is based on a randles equivalent circuit [12]. Nguyen and white proposed a mathematical model of a hermetically sealed lead–acid cell. This model used to study the effect of having an excess negative electrode and the transport rate of oxygen across the separator on the oxygen evolution at the positive electrode and the reduction of oxygen at the negative electrode during charge and overcharge [13]. Gu et al. proposed a three-phase, electrochemical and thermal-coupled model for lead–acid battery. Physical phenomena such as gas generation, transport and electrolyte displacement are incorpo-

---

* Corresponding author.
E-mail address: hejabi_m@alum.sharif.edu (M. Hejabi).

Nomenclature

C_{ad}, C_{dl} absorption capacitance and double layer capacitance (F cm^{-2})

F Faraday constant, 96,487 C mol^{-1}

i, i_0 current density and exchange current density (A cm^{-2})

J $\sqrt{-1}$

k_1, k_{-1} forward and backward rate constant of charge-transfer reaction (cm s^{-1})

R_S, R_{Ct}, R_{ad} solution resistance, charge-transfer resistance, adsorption resistance (Ω cm^2)

SOC   state-of-charge

Z_{Ct} charge-transfer impedance

Z_t total impedance

Z_w Warburg impedance

α, β symmetry factor in the reduction and oxidation direction

θ, Γ coverage degree of adsorbed Pb^{2+} and maximum degree of adsorbed Pb^{2+} (mol cm^{-2})

σ impedance coefficient of Pb^{2+} diffusion

ω angular frequency of ac signal

Superscripts

$\rightarrow$, $\leftarrow$ reduction and oxidation direction

$-$, $\sim$ dc and ac signal

rated in this model [14]. Andersson et al. used a model for porous electrodes to analyze impedance data in such a way that physical parameter can be evaluated. It is also suggested that these parameters can be used as a way of determining the state of health of a battery during float charging [15]. Gu and Nguyen develop a mathematical model of a lead–acid battery, which includes the modeling of porous electrodes and various physical phenomena. The model is used to study the dependence of the performance of the cell on electrode thicknesses and operating temperature [16].
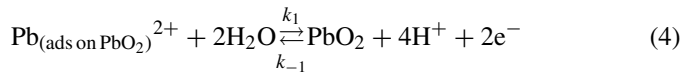
For an accurate model of any electrochemical device, one might employ a rigorous theory taking all the factors into consideration, but in practice that becomes too complicated. Therefore, an equivalent circuit may be used to relate the dynamical behavior of a battery [17]. An equivalent circuit model is an interconnection of electrical elements introduced to represent terminal characteristics of the battery. Such models have been described by a number of scientists including Hampson et al. [18], Willihnganz and Rohner [19] and De Bardelaben [20]. However, they have not considered the relation between these elements (resistance, capacitance, inductance, Warburg impedance, etc.) with various parameter of battery such as concentration of electrolyte, temperature, diffusion coefficient, SOC, rate constant, etc. In this study, the effect of these parameters on Nyquist plot (imaginary part versus real part) has been investigated.

2. Impedance modeling of charge reaction of the lead dioxide electrode

During the discharge of a lead–acid battery, the lead sulfate forms a passive layer on the surface of positive electrode, i.e.

$$PbSO_4 + 2H_2O \rightarrow PbO_2 + 4H^+ + SO_4^{2-} + 2e^- \tag{1}$$
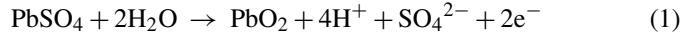
The layer of PbSO$_4$ that is near the surface of the electrode is insulator for electron transfer and it can transmit only ions such as Pb^{2+} and H$^+$. In other words, it is a selective membrane for diffusion of ions. The growth of PbO$_2$ is determined by the flow of Pb^{2+} ions. The Pb^{2+} ions move by surface diffusion along the PbSO$_4$ crystal surface toward the PbO$_2$ phase, where they are oxidized. Considering the above discussion, the following mechanism for the charge process in the positive electrode is suggested [21]:

$$PbSO_4 \underset{k_{-2}}{\overset{k_2}{\rightleftharpoons}} Pb_{(film)}^{2+} + SO_4^{2-} \tag{2}$$

$$Pb_{(film)}^{2+} \xrightarrow{J} Pb_{(ads\ on\ PbO_2)}^{2+} \tag{3}$$

$$Pb_{(ads\ on\ PbO_2)}^{2+} + 2H_2O \underset{k_{-1}}{\overset{k_1}{\rightleftharpoons}} PbO_2 + 4H^+ + 2e^- \tag{4}$$

In the first step, PbSO$_4$ dissolved and the lead ions (Pb^{2+}) are formed in the electrolyte solution near the electrode. In the second step, the lead ions diffused in lead sulfate layer and adsorption of (Pb^{2+}) ions takes place. Finally, the adsorbed ions convert to lead dioxide (PbO$_2$) during the charge-transfer reaction. In order to analyze and interpret the electrochemical behavior of such a reaction, it is necessary to derive a theoretical expression for the impedance of the above process.

The current density for the charge-transfer step (reaction (4)) can be expressed as follows:

$$i = \vec{i} - \overleftarrow{i} = nF \left[k_1 \theta a_{H_2O}^2 \exp\left(-\frac{\alpha nF\varphi}{RT}\right) \right.$$
$$\left. - k_{-1}(1-\theta) a_{H^+}^4 \exp\left(\frac{\beta nF\varphi}{RT}\right) \right] \tag{5}$$

In ac impedance studies, the variables are composed of a steady-state component plus an alternating component:

$$i = \bar{i} + \tilde{i}, \quad \theta = \bar{\theta} + \tilde{\theta}, \quad \varphi = \bar{\varphi} + \tilde{\varphi} \tag{6}$$

Differentiation of Eq. (5) gives:

$$\frac{d\tilde{i}}{dt} = nF\left[-\left(\frac{\vec{i}}{\theta nF} + \frac{\overleftarrow{i}}{(1-\theta)nF}\right)\frac{d\tilde{\theta}}{dt} \right.$$
$$\left. - \frac{1}{RT}(\alpha\vec{i} + \beta\overleftarrow{i})\frac{d\tilde{\varphi}}{dt} \right] \tag{7}$$

where $\tilde{i}$, $\tilde{\theta}$ and $\tilde{\varphi}$ are at the same frequencies as expressed by

$$\tilde{L} = L_0 \exp(j\omega t) \tag{8}$$

in which $\tilde{L}$ represents $\tilde{i}$, $\tilde{\theta}$, $\tilde{\varphi}$ and L_0 are the amplitude of these variables. The time derivative of Eq. (8) is

$$\frac{\mathrm{d}\tilde{L}}{\mathrm{d}t} = j\omega\tilde{L} \tag{9}$$

Thus Eq. (7) can be further simplified as follows:

$$\tilde{i} = -\left[\frac{\vec{i}}{\theta} + \frac{\leftarrow i}{(1-\theta)}\right]\tilde{\theta} - \frac{nF}{RT}(\alpha\vec{i} + \beta\leftarrow i)\tilde{\varphi} \tag{10}$$

The interfacial impedance of the lead dioxide electrode (Z) is expressed by:

$$Z = -\frac{\tilde{\varphi}}{\tilde{i}} \tag{11}$$

From the above equation, one can obtain the following relation:

$$Z = Z_F + Z_t \tag{12}$$

where

$$Z_F = \frac{RT}{nF(\alpha\vec{i} + \beta\leftarrow i)} = R_{ct} \tag{13}$$

And

$$Z_t = \frac{RT}{nF(\alpha\vec{i} + \beta\leftarrow i)}\left[\frac{\vec{i}}{\theta} + \frac{\leftarrow i}{(1-\theta)}\right]\frac{\tilde{\theta}}{\tilde{i}} \tag{14}$$

where $Z_F = R_{ct}$ is the impedance due to the charge-transfer reaction and Z_t is the impedance due to diffusion and adsorption of lead ions. Therefore, the contribution to the impedance is due to these steps: charge-transfer reaction, diffusion of Pb^{2+}, adsorption of Pb^{2+}, which is described by Eqs. (3) and (4).

Consider Eq. (5) being at equilibrium:

$$\vec{i} = \leftarrow i = i_0 = nFk_1\bar{\theta}a_{H_2O}^2 \exp\left(\frac{-\alpha nF}{RT}\varphi\right)$$

$$= nFk_{-1}a_{H^+}^4(1-\bar{\theta})\exp\left(\frac{\beta nF}{RT}\varphi\right) \tag{15}$$

Let

$$\alpha = 0.5, \qquad \beta = 0.5, \qquad \bar{\theta} \gg \tilde{\theta} \tag{16}$$

$$A = \frac{a_{H_2O}^2}{a_{H^+}^4} \exp\left[\frac{nF}{RT}\varphi\right] \tag{17}$$

$$K_1 = \frac{k_1}{k_{-1}} \tag{18}$$

Combining Eqs. (15)–(18), and assuming $a_{H^+} = C_{H^+}$, Z_F and Z_t can be obtained as follows:

$$Z_F = R_{ct} = \frac{RT}{nFi_0} = R_{ct} = \frac{RT(1+K_1A)}{n^2F^2k_{-1}C_{H^+}^4 \exp((\beta nF/RT)\varphi)} \tag{19}$$

And

$$Z_t = \frac{RT}{nF\bar{\theta}(1-\bar{\theta})}\frac{\tilde{\theta}}{\tilde{i}} = \frac{RT(1+K_1A)^2}{nFK_1A}\frac{\tilde{\theta}}{\tilde{i}} \tag{20}$$

In order to obtain $\tilde{\theta}/\tilde{i}$, reactions (2) and (3) are taken into account and we can introduce some parameters which depend on diffusion and adsorption:

$$PbSO_4 \underset{k_{-2}}{\overset{k_2}{\rightleftarrows}} Pb^{2+} + SO_4^{2-} \tag{21}$$

And we obtain:

$$\tilde{i} - nFk_2\theta(1-\chi_s) - nFJ + nFk_{-2}\chi_s(1-\theta) = nF\Gamma\frac{\mathrm{d}\theta}{\mathrm{d}t} \tag{22}$$

By separating the alternate parts and dc parts we obtained $\bar{\chi}_s$ and $\tilde{\chi}_s$:

$$\bar{\chi}_s = \frac{k_2\bar{\theta}}{k_2\bar{\theta} + k_{-2}(1-\bar{\theta})} \tag{23}$$

According to mass balance at the electrode surface:

$$\tilde{i} - nF\Gamma j\omega\tilde{\theta} = nF\tilde{j}_i \tag{24}$$

And

$$\tilde{j}_i = N\tilde{\chi}_s F(j\omega, D) \tag{25}$$

By using Eqs. (24) and (25) we can obtain $\tilde{\chi}_s$:

By substitution $\tilde{\chi}_s$ and $\bar{\chi}_s$ we obtain $\tilde{\theta}/\tilde{i}$

With considering the resistance of solution R_s and a double layer capacitance C_{dl}, the total impedance of the lead dioxide electrode is

$$Z_{total} = R_s + \frac{1}{j\omega C_{dl} + (1/R_{ct} + (1/j\omega c_{ad} + (1/Z_d)))} \tag{26}$$

$$R_{ct} = \frac{RT(1+K_1A)}{n^2F^2k_{-1}C_{H^+}^4 \exp((\beta nF/RT)\varphi)} \tag{27}$$

$$C_{ad} = \frac{n^2F^2\Gamma}{RT}\left[\sqrt{K_1A} + \frac{1}{\sqrt{K_1A}}\right]^{-2} \tag{28}$$

$$\sigma = \frac{RT}{nFN}(1 + K_1K_2A) \tag{29}$$

$$Z_d = \left[\frac{\sigma}{\sqrt{\omega D_n^2}}\right](1-J)\left[\tan h\left(\delta\sqrt{\frac{j\omega}{D_n}}\right)\right] \tag{30}$$

The equivalent circuit corresponding to Eq. (26) is shown in Fig. 1, which is the total impedance of lead dioxide electrode in lead–acid battery neglecting gas evolution.
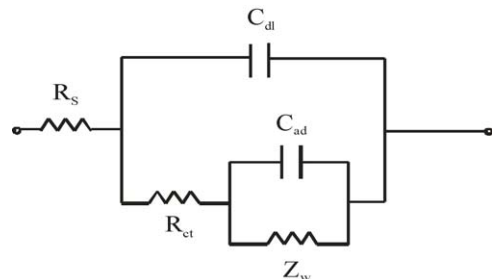

Fig. 1. Equivalent circuit for lead dioxide electrode in lead–acid battery during charge reaction.

3. Experimental setup

A cell is used for this test that consists of one half positive plate and two negative plates (that pasting, curing, charging previously) of a 6SB3 motorcycle MF battery. The electrolyte is sulfuric acid with specific gravity of 1.28.

The charge/discharge and impedance data are obtained with SOLARTON 1470, a multi-channel battery tester system. Frequencies of the impedance spectroscopy are swept from l00 kHz to 1 mHz at amplitude of 10 mV. All cells are tested in 2nd cycle of charge/discharge. During second discharge cycle the impedance spectroscopes are performed in under zero current in 10 different SOC (100–10%) for measurement in different potential.

4. Results and discussion

R_{ct} is the charge-transfer resistance and depends on parameters such as T, k_1, k_{-1}, ϕ and C_{ad}, the capacitance due to adsorption, depends on T, Γ, n, k_1 and k_{-1}. Z_w is the Warburg impedance due to the mass transfer of ions in PbSO$_4$ film whose effects appears in the low frequency region. With change of some parameters, some component (R_{ct}, C_{ad}, Z_w, etc.) in a specific frequency range shows their alter effect to the general form of curves. Fig. 2 represents the effect of diffusion coefficient of (Pb^{2+}) ions on Nyquist curves. As shown in Fig. 2 with the decrease of $Dn_{Pb^{2+}}$, the magnitude of the impedance increases. According to the derived equations, the effect of $Dn_{Pb^{2+}}$ is considerable in Warburg impedance and with increase in the density of system, the amplitude of $Dn_{Pb^{2+}}$ decreases. For instance when we apply a gelled electrolyte in lead–acid battery or during charge/discharge cycles, the thickness and the density of PbSO$_4$ layer increase.

Theoretical results of Fig. 3 show that acid concentration influence on Nyquist plots and the most effect is on charge-transfer stage. By considering experimental results of different SOCs, we obtain that some changes in SOC cause changes in charge-transfer part. By comparison two Figs. 3 and 4 we can see
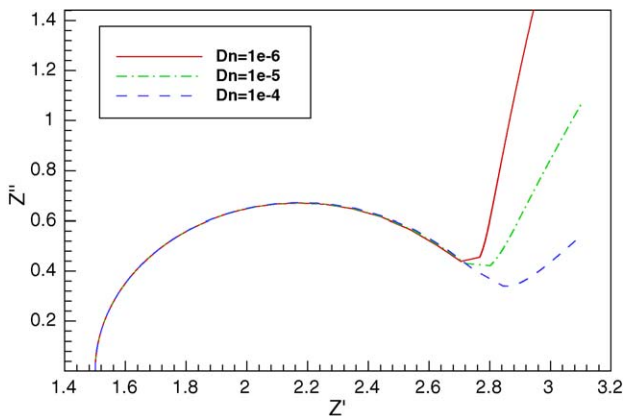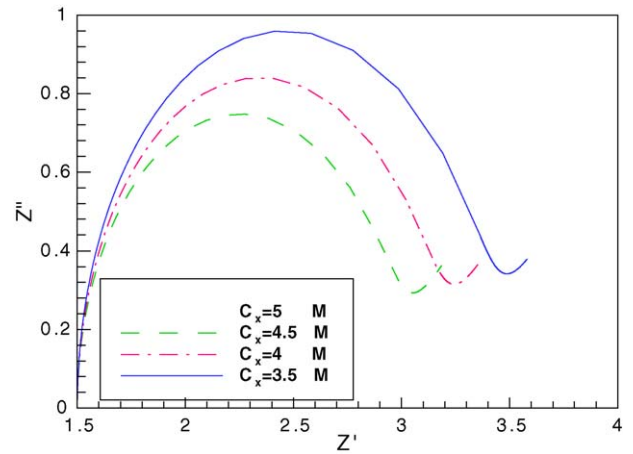

Fig. 3. Nyquist plots for lead electrode during charge reaction simulated based upon (26) at different $C_x = C_{H^+}^4$, with parameters of, $T = 300$, $C_{dl} = 9 \times 10^{-6}$ F cm^{-2}, $R_s = 1.5$ ohm cm^2, $\Gamma = 1 \times 10^{-6}$ mol cm^{-2} and $k_1 = 1 \times 10^{-4}$ cm s^{-1}.
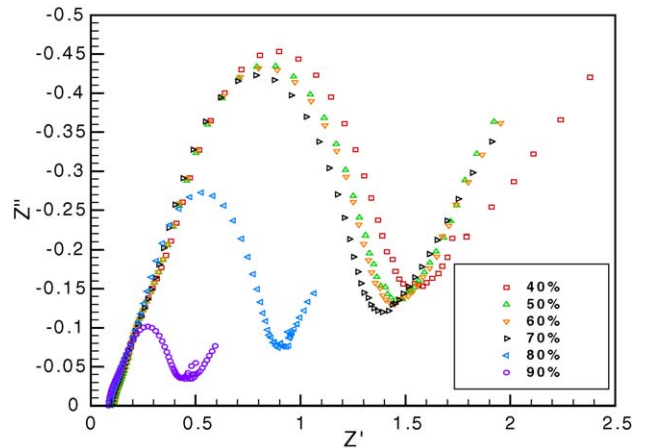

Fig. 4. Nyquist plots for positive electrode in lead–acid battery during discharge reaction based upon experimental results at different SOC.

a direct relation between acid concentration and SOC, as a result, although other parameters too have an effect on SOC also. For example, PbSO$_4$ thickness change shows its influence on mass transfer part. Because of the purpose of reviewing one by one

Fig. 2. Nyquist plots for positive electrode in lead–acid battery during charge reaction simulated based upon Eq. (26) at different $D_{Pb}{}^{2+}$, with parameters of, $C_x = 5$ M, $k_1 = 1 \times 10^{-4}$ cm s^{-1}, $C_{dl} = 9 \times 10^{-6}$ F cm^{-2}, $R_S = 1.5$ Ω cm^2, $\Gamma = 1 \times 10^{-6}$ mol cm^{-2} and $T = 300$ K.
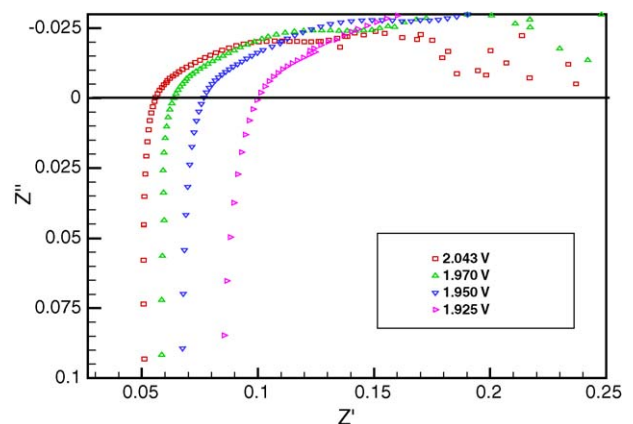

Fig. 5. Nyquist plots for positive electrode in lead–acid battery during discharge reaction based upon experimental results at different potential.

of parameter on cell characteristics, we consider the changes of parameters separately.

As Fig. 5 depicts, R_s changes cause the potential variation. It appears that the study of the impedance modeling of the positive electrode could supply valuable information for elucidating the dynamics of the processes taking place in lead–acid battery. Our model is a simple model and the parameters such as porosity factor, surface adsorption effects, etc. are not involved in our modeling and only simple electrochemical reaction and mass transfer equations are used for description of system in contrast to the other papers, but eventually it provides acceptable results.

5. Conclusion

1. Direct relation between SOC and acid concentration.
2. Reverse relation between R_s and terminal's voltage.
3. R_{ct} and C_{ad} depend on parameter such as T, k_1, φ, C_{H^+},..., etc.
4. The comparison between experimental and theoretical results show that components of this model are functions of battery properties such as diffusion coefficient, temperature and rate constant.

Acknowledgments

References

[1] Y. Nakagama, K. Kishimoto, S. Sugiyama, S. Sakaguchi, J. Power Sources 107 (2002) 192–200.
[2] S.S. Misra, T.M. Noveske, S.L. Mraz, A.J. Williamson, J. Power Sources 95 (2001) 162–173.
[3] C.D. Parker, J. Power Sources 100 (2001) 18–28.
[4] J. Crew, I. Francis, P. Butler, J. Power Sources 95 (2001) 241–247.
[5] A.J. Salkind, C. Fennie, P. Singh, T. Atwater, D.E. Reisner, J. Power Sources 80 (1999) 293.
[6] A. Salkind, T. Atwater, P. Singh, S. Nelatury, S. Damodar, C. Fennie Jr., D. Reisner, J. Power Sources 96 (2001) 151.
[7] F. Huet, J. Power Sources 70 (1998) 59–69.
[8] S. Buller, M. Thele, E. Karden, R.W. De Doncker, J. Power Sources 113 (2003) 422.
[9] Z. Stoynov, B. Savova-Stoynov, T. Kossev, J. Power Sources 30 (1990) 275.
[10] A. Tenno, R. Tenno, T. Suntio, J. Power Sources 111 (2002) 65–82.
[11] A. Tenno, R. Tenno, T. Suntio, J. Power Sources 103 (2001) 42–53.
[12] P. Mauracher, E. Karden, J. Power Sources 67 (1997) 69–84.
[13] T.V. Nguyen, R.E. White, Electrochim. Acta 38 (1993) 935–945.
[14] W.B. Gu, G.C. Wang, C.Y. Wang, J. Power Sources 108 (2002) 174–184.
[15] H. Andersson, I. Pteresson, E. Ahlberg, J. Appl. Electrochem. 31 (2001) 1.
[16] H. Gu, T.V. Nguyen, J. Electrochem. Soc. 134 (1987) 2953–2960.
[17] S.R. Nelatury, P. Singh, J. Power Sources 132 (2004) 309–314.
[18] N.A. Hampson, et al., J. Appl. Electrochem. 10 (1980) 3–11.
[19] E. Willihnganz, P. Rohner, Electr. Eng. 78 (9) (1959) 922–925.
[20] S. De Bardelaben, Determining the End of Battery Life, INTELLEC 86, IEEE Publication, 1986, pp. 365–386.
[21] D. Pavlov, Z. Diner, J. Electrochem. Soc.: Electrochem. Sci. Technol. 127 (4) (1980) 855–863.